COBEM 2023 27TH INTERNATIONAL CONGRESS OF MECHANICAL ENGINEERING

ABCM Brazilian Society of Mechanical Sciences and Engineering
27th ABCM International Congress of Mechanical Engineering
December 04-08, 2023, Florianópolis-SC, Brazil

COB-2023-1006
NUMERICAL ANALYSIS OF THE EFFECTS OF CONVERGENT-DIVERGENT NOZZLE GEOMETRY ON THE CHARACTERISTICS OF SUPERSONIC JET IN BOF CONVERTERS.

Pedro Francelino Garcia
Ayrton Cavallini Zotelle
Renato do Nascimento Siqueira
João Paulo Barbosa
LPMF, Department of Mechanical Engineering, Instituto Federal do Espírito Santo - campus São Mateus, Rod. BR 101 norte, km 58, Litorâneo, São Mateus, ES, 29932-540, Brazil
pedrogfrancelino@gmail.com
ayrton.zottele@ifes.edu.br
renatons@ifes.edu.br
jpbarbosa@ifes.edu.br

Breno Totti Maia
Lumar Metalúrgica LTDA
breno.totti@lumarmetals.com.br

José Roberto de Oliveira
Instituto Federal do Espírito Santo
jroberto@ifes.edu.br

Abstract. *Convergent-divergent nozzles are widely used in Basic Oxygen Furnaces (BOF) to accelerate oxygen to supersonic speeds, enabling the decarburization process of the hot metal. New nozzle geometries hold promise for enhancing the efficiency of steelmaking process. In this study, it was analyzed the trapezoidal, ideal, ideal truncated at different proportions (7.45%, 14.9%, 22.35%, and 29.8%), and ideal compressed geometries, using Computational Fluid Dynamics (CFD) with two-dimensional axisymmetric modeling and the SST k-w turbulence model, considering the fluid as an ideal gas. The results revealed that truncating the geometry increases the intensity of shocks at the nozzle exit, while compression intensifies shocks in the throat region. Additionally, all the truncated, compressed, and ideal geometries exhibited a larger potential core compared to the trapezoidal geometry. It was observed that truncating and compressing the divergent region by 29.8% of the initial length resulted in more significant losses in the velocity and length of the potential core compared to the ideal geometry. These findings suggest that modifying the nozzle geometry can play a crucial role in improving the performance of the steel manufacturing process.*

Keywords: *Supersonic Nozzle, Computational Fluid Dynamics, Shock waves, Method of characteristics, Basic oxygen process.*

1. INTRODUCTION

The use of steel in various applications has been steadily increasing, resulting in a growing demand for more production. According to Garajau et al. (2017), the need to produce high-quality and cost-effective steel has become a "rule" imposed by the market in recent years, due to fierce competition among global steelmakers.

Currently, the majority of steel produced worldwide undergoes a refinement process known as the "Basic Oxygen Process" (BOF), illustrated in Figure 1a. This method involves injecting oxygen at supersonic velocity into the hot metal through a lance (Figure 1b) and a compressor to deoxidize the metal and transform it into liquid steel (FRUEHAN, 1998).

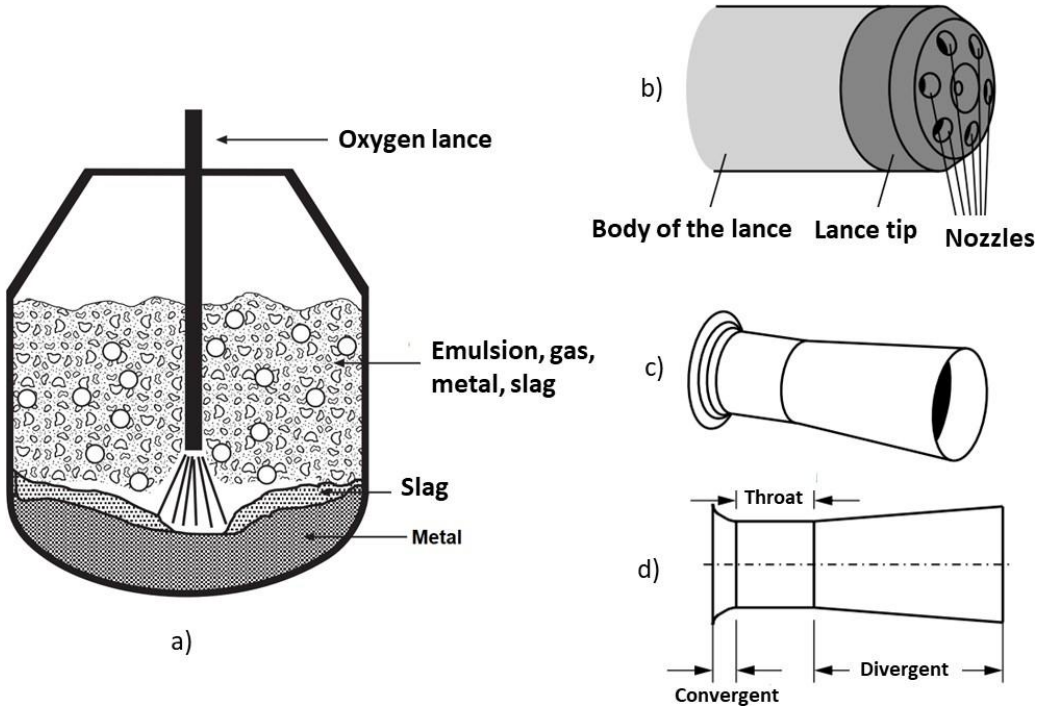

Figure 1. Exemplification of a refining process using a BOF converter. Legend: (a) Interaction of metal, slag, and emulsion inside the converter (FRUEHAN, 1998), (b) Body and lance tip with 6 nozzles, (c) Isometric view of the trapezoidal nozzle, (d) Orthographic view of a nozzle and its convergent, throat, and divergent sections (STORCH, 2017).

Supersonic flow occurs due to the convergent-divergent geometry of the nozzle (Figure 1c). The flow characteristics will depend on the operating conditions in which the nozzle is immersed, such as the inlet pressure of the nozzle (P_{in}) and the ambient pressure (P_a) of the converter. The ratio between P_{in} and P_a is known as the Nozzle Pressure Ratio (NPR), as stated by Eq. (1).

$$NPR = \frac{P_{in}}{P_a} \tag{1}$$

The geometry of the nozzle plays a fundamental role in the steelmaking process. Specifically, the shape of the divergent part of the nozzle has a direct impact on the process efficiency. Inadequate sizing in these regions can lead to an increase in the time required for steel production (SILVEIRA, 2019).

Most nozzles used in BOF converters adopt the trapezoidal geometry, as illustrated in Figure 1d. However, other geometries, mainly derived from the aerospace industry, have been explored. Ostlund et al. (2005) mentions, in addition to the trapezoidal geometry, the use of the ideal geometry, which allows supersonic flow without the formation of shock waves (which can impair the process and the nozzle's lifespan). Furthermore, the ideal truncated and ideal compressed geometries are also mentioned with the aim of reducing the dimensions of the ideal geometry, which has an elongated length.

Indeed, with the increasing demand for more production, the implementation of improvements in the BOF process, and studies on modifying the nozzle geometry, emerges as a promising area of development. A reduction of one minute in the steel manufacturing time can result in annual gains of thousands of dollars (MAIA, 2007).

2. MATHEMATICAL EQUATIONS

The problem formulation is a steady, compressible, and turbulent flow on a nozzle, modelled by the unsteady Reynolds Averaged Navier-Stokes (RANS) formulation (ANSYS, 2013). The continuity equation is:

$$\frac{\partial}{\partial x_i}(\rho u_i) = 0, \tag{2}$$

where ρ and u_i are the density and velocity field in the i^{th} direction, respectively. The momentum equation for the proposed problem is:

$$\frac{\partial}{\partial \mathrm{x}_i}\left(\rho u_i u_j\right) = -\frac{\partial \mathrm{P}}{\partial \mathrm{x}_i} + \frac{\partial}{\partial \mathrm{x}_j}\left[(\mu + \mu_t)\left(\frac{\partial u_i}{\partial \mathrm{x}_j} + \frac{\partial u_j}{\partial \mathrm{x}_i} - \frac{2}{3}\frac{\partial u_i}{\partial \mathrm{x}_i}\delta_{ij}\right)\right], \tag{3}$$

in which P is the pressure field of the fluid, μ is the fluid viscosity, μ_t is the turbulent viscosity, and δ_{ij} the Kronecker delta function. An essential description for compressible flows is how the density field is determined. The fluid density is calculated on the numerical domain by:

$$\rho = \rho_0 \left(1 + \frac{\mathrm{K} - 1}{2} Ma^2\right)^{\frac{1}{1-k}}, \tag{4}$$

where ρo is the density of the fluid at ambient temperature (300 K) and $Ma = u/c$, is the Mach number. The sound velocity is given by $c = \sqrt{\gamma RT}$, in which R is the gas constant, γ the specific heat ratio and T the temperature field, determined solving the energy equation though the numerical domain:

$$\frac{\partial}{\partial \mathrm{x}_i}\left[\rho\left(c_p u_i T + \frac{{u_i}^2}{2}\right)\right] = (K + K_t) - \frac{\partial^2 \mathrm{T}}{\partial {\mathrm{x}_i}^2} + \frac{\partial}{\partial \mathrm{x}_i}\left[\mu\left(\frac{\partial u_i}{\partial \mathrm{x}_j} + \frac{\partial u_j}{\partial \mathrm{x}_i} - \frac{2}{3}\frac{\partial u_i}{\partial \mathrm{x}_i}\delta_{ij}\right)u_i\right], \tag{5}$$

where c_p is the specific heat at constant pressure, K the thermal conductivity of fluid and K_t the turbulent thermal conductivity of fluid. The parameters μ_t and K_t were obtained by the application of a turbulence closure model.

2.1 Turbulence Model

The SST $k - \omega$ model is widely used in the literature to simulate supersonic flows in Laval nozzles due to its ability to combine the advantages of two models, using the $k - \omega$ model near the wall and the $k - \varepsilon$ model in the rest of the domain (HADJADJ et al., 2015; ALLAMAPRABHU et al., 2016; LI et al., 2015). In this model, the turbulent viscosity is given by $\mu_t = \rho \sigma_t k/\omega$ and the thermal conductivity by $K_t = K\mu_t/\mu$, where σ_t is a model constant. The turbulent kinetic energy (k) and the specific dissipation rate (ω) were calculated as:

$$\frac{\partial}{\partial \mathrm{x}_i}(\rho k u_i) = \frac{\partial}{\partial \mathrm{x}_j}\left[\left(\mu + \frac{\mu_t}{k}\right)\frac{\partial k}{\partial \mathrm{x}_j}\right] + G_k - Y_k, \tag{6}$$

$$\frac{\partial}{\partial \mathrm{x}_j}\left(\rho \omega u_j\right) = \frac{\partial}{\partial \mathrm{x}_j}\left[\left(\mu + \frac{\mu_t}{k}\right)\frac{\partial \omega}{\partial \mathrm{x}_j}\right] + G_\omega - Y_\omega + D_\omega. \tag{7}$$

For those equations, σ_k, and σ_ω are empirical constants of the model for k, and ω, respectively. G_k is the production of turbulence kinetic energy, G_ω the generation of ω, and Y_k and Y_ω are the dissipation of k and ω due to turbulence and D_ω represents the cross-diffusion term (ANSYS, 2013). The constants used (σ_t, σ_k and σ_ω) were the default values of ANSYS Fluent 2022.

3. METHODOLOGY

The numerical simulation setup considered a two-dimensional geometry with an axis of symmetry, as illustrated in Figure 2a. In this figure, it is possible to visualize the plane which, when revolved, forms the convergent-divergent nozzle. Based on the trapezoidal geometry proposed by ZAPRYAGAEV (2002), the geometry was constructed for numerical simulation (Figure 2b). This geometry was used to perform mesh testing and validate the solution. From the trapezoidal geometry, the other nozzles were constructed, keeping the approach region and the convergent region, with modifications made to the contour of the divergent region (Figure 2c).

In Figure 2a, it is possible to observe that not only the nozzle is modeled in the geometry but also the surrounding environment. As a metric, following the approach used by Storch (2017), the total length of the geometry was defined as 70 times the exit diameter of the nozzle, while the height of the geometry corresponds to 15 times the exit diameter of the nozzle. These proportions are used to ensure an adequate representation of the geometry and its spatial context.

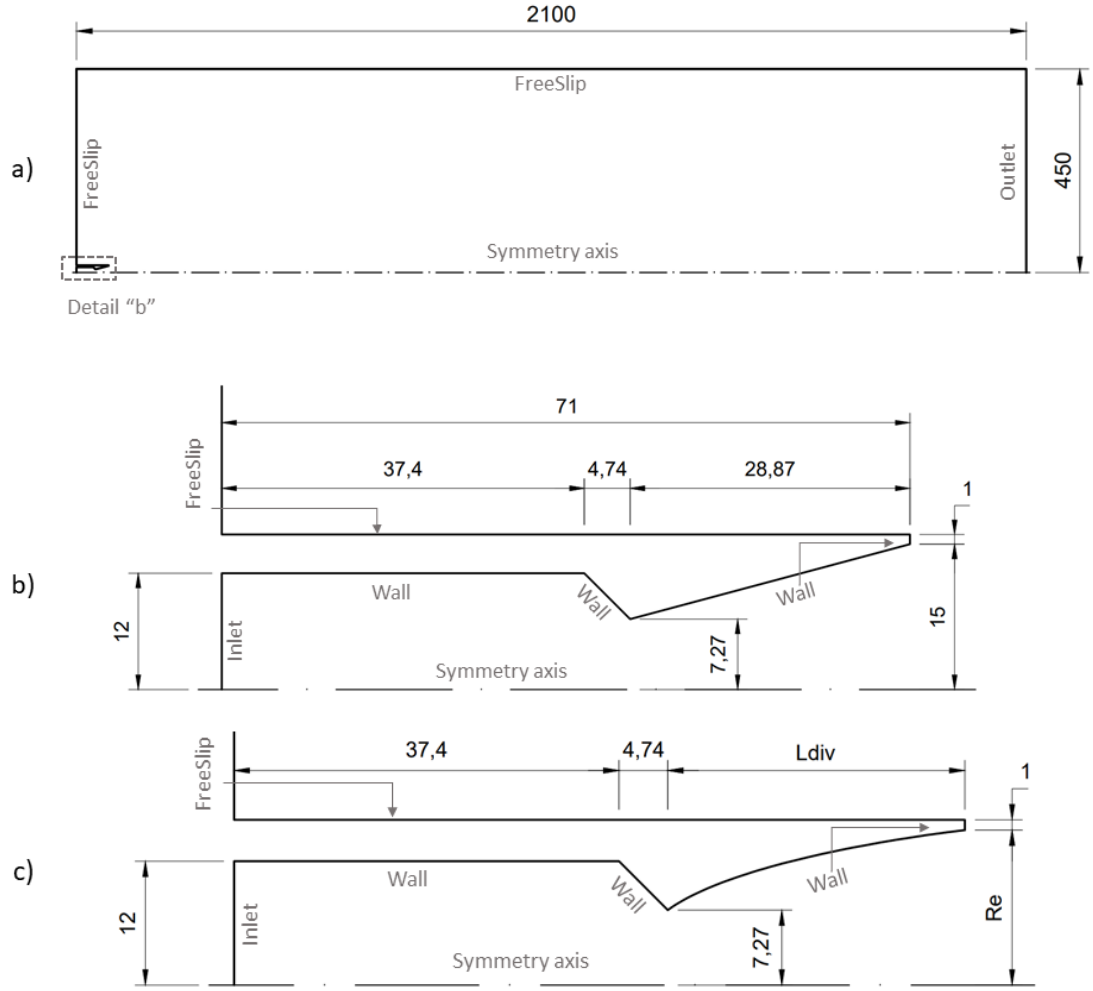

Figure 2. Geometry of the nozzles and boundary conditions. Legend: (a) Overall view of the geometry, (b) Details of the trapezoidal nozzle, (c) Details of the curvilinear nozzles, "Ldiv" length of the divergent region of the curvilinear nozzles, "Re" exit radius of the curvilinear nozzles.

The contours of the curvilinear nozzles in Figure 4.2c were obtained using MATLAB software, version 2022. In this process, the algorithms called "Supersonic Nozzle Design Tool" and "Minimum Length Nozzle Design Tool" were used, which were developed by Cory Dodson (2023). These algorithms are based on the Method of Characteristics (MOC) presented by Andersson (2021). The codes are available in the online files of the MathWorks company.

For the mesh, the multizone method was used, where a lower level of refinement was chosen for the region far from the nozzle, aiming to reduce computational cost, as shown in Figure 3a. On the other hand, a higher level of refinement was selected for the nozzle and the region where the potential core can develop (Figure 3b).

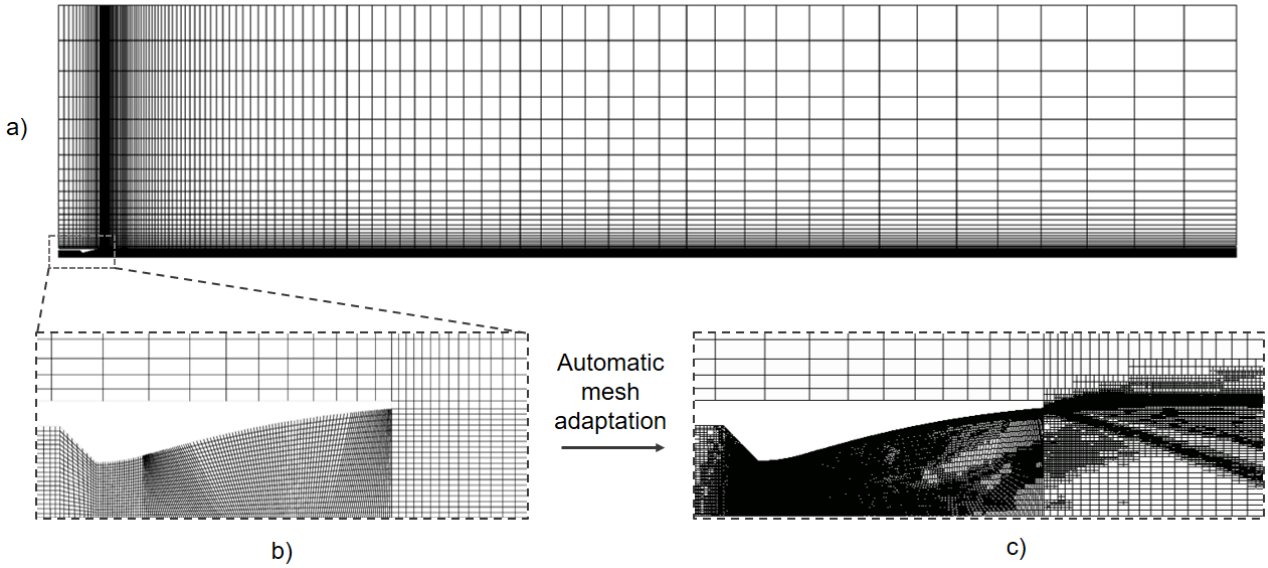

Figure 3. Computational domain mesh. Legend: (a) general aspect of the base meshes for all geometries, (b) detail of the refinement inside and around the nozzle, (c) automatic refinement by density gradient.

The initial base mesh had 7693 nodes and 7422 elements. To better characterize the structures of the supersonic flow and obtain an independent mesh solution, it was necessary to add an automatic adaptive mesh with a density refinement criterion, with 4 levels of refinement, as shown in Figure 4.5c. The adaptive mesh used is based on density refinement (dominant hexahedral mesh method, cut-cell), which refines the mesh in regions where the density gradient is high, subdividing the initial element into 2^{2n} elements, where n represents the refinement level.

The configurations used in the numerical solution set in ANSYS Fluent version 2022 can be observed in Table 1. Additionally, the atmospheric pressure is set at 1 bar, the design Mach number for each nozzle is 3, and the specific heat ratio for air is 1.4.

Table 1. Settings for numerical simulation.

Material	Density at ambient temperature		1.225 kg/m³
	Specific heat		1006.43 J/(kg K)
	Viscosity		1.7894 kg/(m s)
	Molar mass		28.966 kg/kmol
Methods	Pressure-Velocity Coupling		Coupled
	Spatial discretization	Gradient	Least Squares Cell Based
		Pressure	Second Order
		Momentum	First Order Upwind
		Density	Second Order
		Energy	Second Order Upwind
		Turbulent kinetic energy	Second Order Upwind
		Specific dissipation rate	Second Order Upwind

4. RESULTS AND DISCUSSIONS

A mesh test was conducted on the geometry proposed by ZAPRYAGAEV (2002), as shown in Figure 4, with the objective of evaluating the effect of mesh refinement. Automatic density-based refinement was used to generate different refinement levels. The numerical simulations were performed starting from the zero-refinement level, without any refinement, up to five levels of refinement.

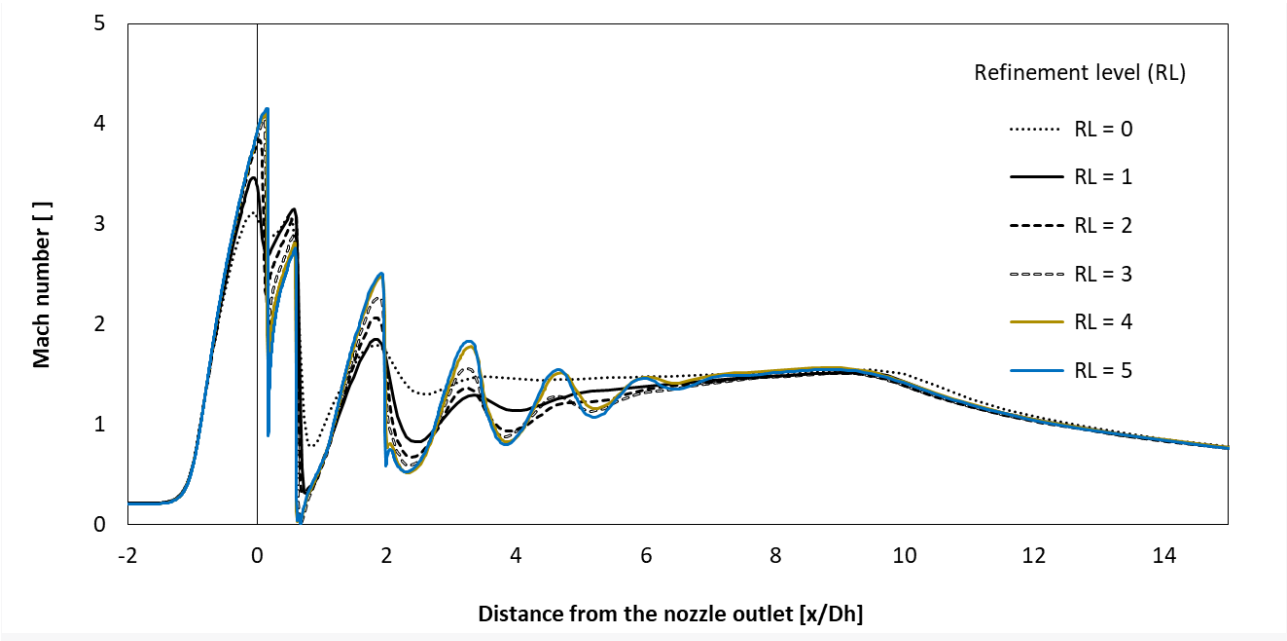

Figure 4. Mesh refinement test using an automatic density gradient-based refinement level for the flow.

The author ZAPRIAGAEV (2002) conducted Schlieren images for various NPR values. In order to validate the numerical experiment, the results obtained by him were compared, as illustrated in Figure 5. The upper images correspond to the practical experiment and the lower images to the numerical simulations.

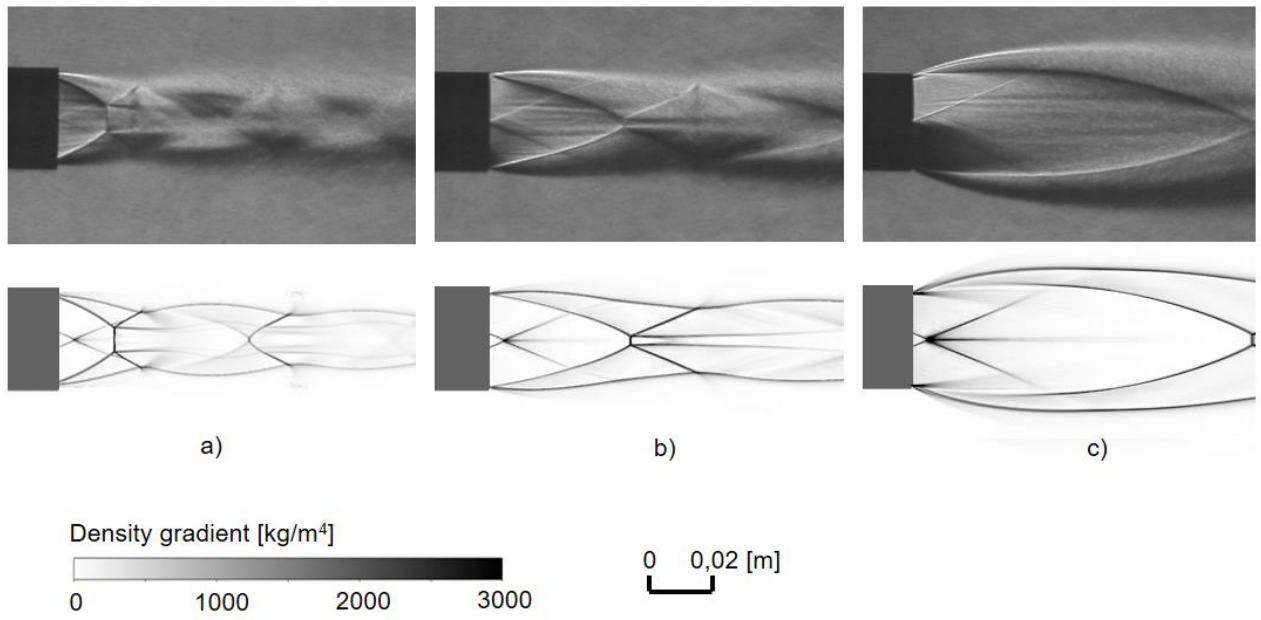

Figure 5. Comparison of numerical results (lower imagens) with the experimental results (upper images) of ZAPRIAGAEV (2002). Legend: (a) NPR = 11.13; (c) NPR = 27.48; (b) NPR = 85.00.

In Figure 5, it can be observed that the structures from both approaches are in agreement, both in terms of shape and length, indicating that the numerical modeling presented is consistent with the experimental results.

The density gradients of nozzles with truncated geometry can be observed in Figure 6. On the left, we find the reference nozzle designed by the method of characteristics (Figure 6a). The geometry truncation occurs progressively (from left to right) as illustrated in Figures 6b to 6e. The rightmost nozzle corresponds to the trapezoidal nozzle of ZAPRYAGAEV (2002). In this figure, it is possible to identify different zones, such as areas where oblique incident shocks (OIS), reflected shocks, and normal shocks (NS) with slip lines occur. Furthermore, as the truncation of the geometry becomes more significant (Figure 6b to 6e), an incident oblique shock from the nozzle exit becomes more intense. This leads to the appearance of a normal shock in Figure 6c, which intensifies in Figures 6d and 6e. Since shockwaves induce significant entropy variation and dissipate energy from the flow, the intensification of oblique shocks and the appearance of the normal shock from Figure 6c tend to indicate that truncations exceeding 14.90% lead to more energy loss. However, it is important to note that even the 29.80% truncation exhibits less intense shockwaves compared to the trapezoidal geometry.

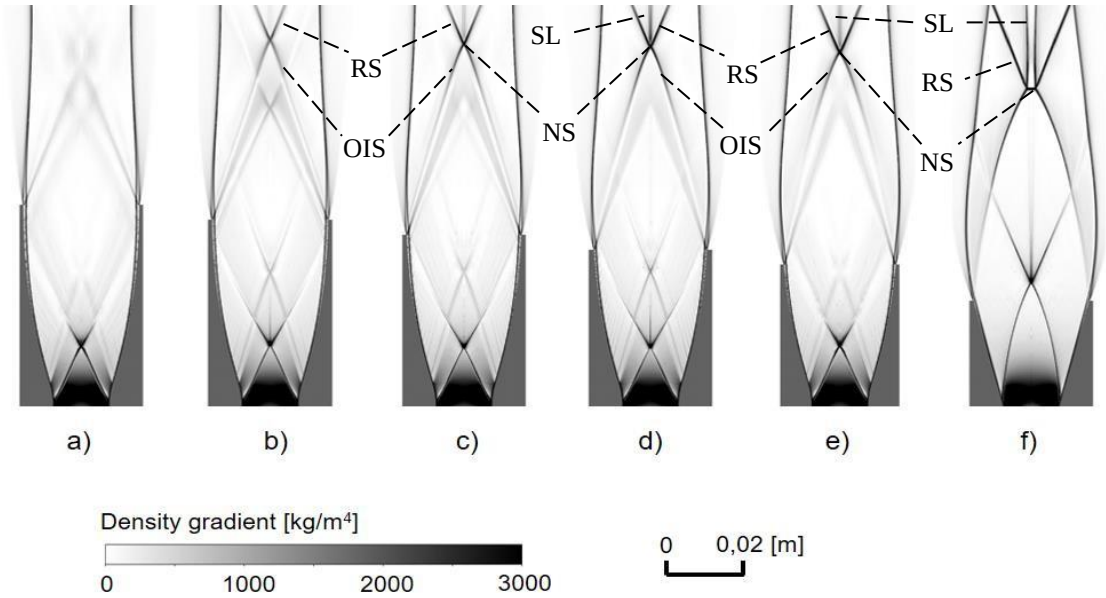

Figure 6. Density gradient in the divergent region of the nozzle and in the region near the exit. Legend: (a) MOC, (b) truncated 7.45%, (c) truncated 14.90%, (d) truncated 22.35%, (e) truncated 29.80%, (f) trapezoidal.

Density gradients in nozzles with compressed geometry are depicted in Figure 7. On the left side, the reference nozzle, designed using the method of characteristics (Figure 7a), is presented. The compression of geometry is demonstrated progressively from left to right in Figures 7b to 7e. The furthest right nozzle corresponds to the trapezoidal nozzle as proposed by ZAPRYAGAEV (2002). In the same manner that the process of geometry truncation led to alterations in the structures of supersonic flow, compression also induces changes. However, contrary to the effect caused by truncation, the compressed geometry amplified the impact of the shocks generated at the throat. As the geometry was compressed, an incident oblique shock (IOS) originating from the throat began to intensify (Figure 7b and 7c). Starting from a compression of 22.35% (Figure 7d), a weak slip line (SL) appears, indicating the emergence of a normal shock (NS) in the flow, which becomes more pronounced in Figure 7e. Generally, the intensification of shock waves within the nozzle is detrimental to its operational lifespan.

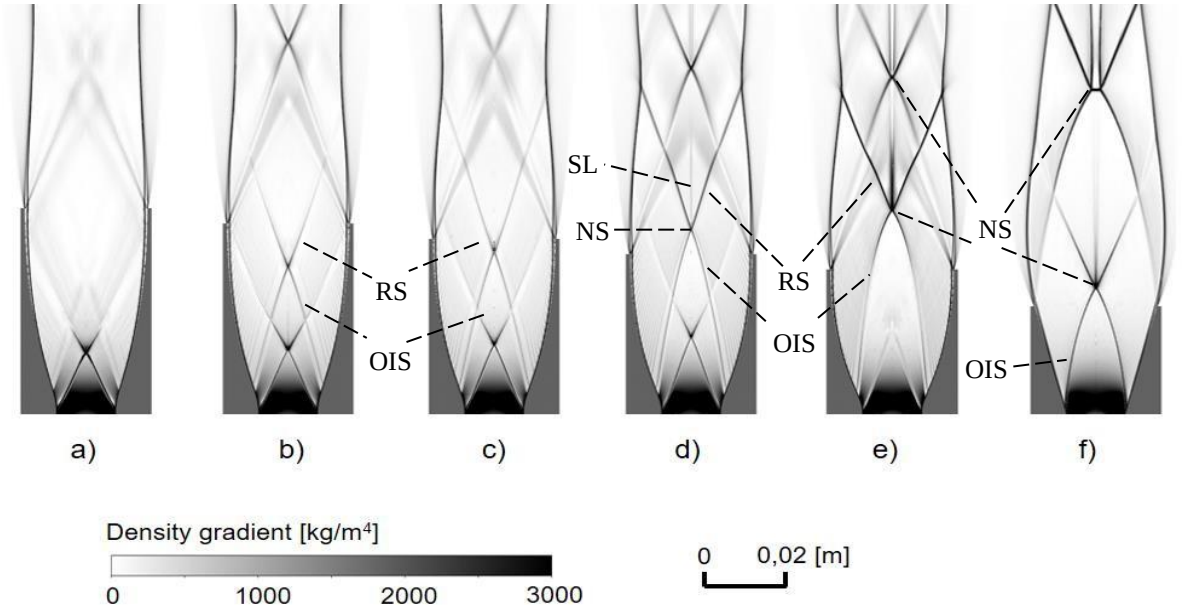

Figure 7. Density gradient in the divergent region of the nozzle and in the region near the exit. Legend: (a) MOC, (b) compressed 7.45%, (c) compressed 14.90%, (d) compressed 22.35%, (e) compressed 29.80%, (f) trapezoidal.

To quantitatively assess the impacts resulting from the truncation and compression of geometries, the Mach number of the potential core of the jet and its length was illustrated in Figure 8. The distance was non-dimensionalized by the throat diameter of the nozzle.

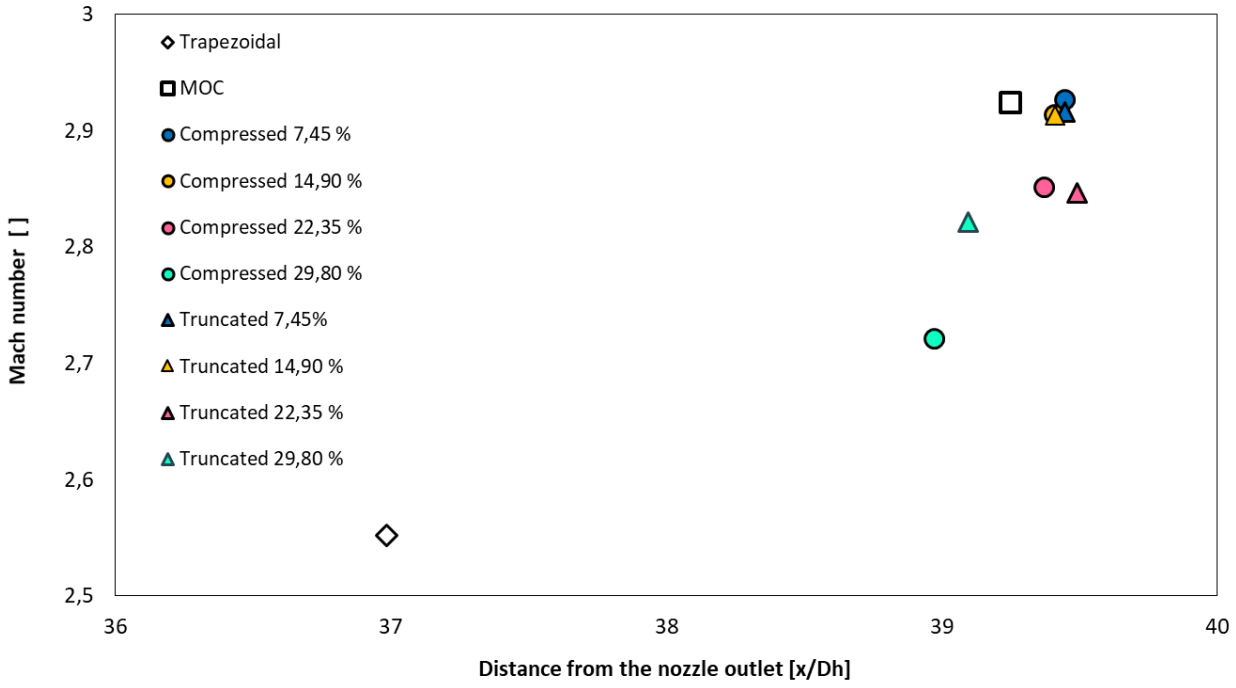

Figure 8. Comparison of the potential core and Mach number for the truncated, compressed, trapezoidal, and MOC geometries.

Comparing the curvilinear geometries among themselves, the MOC, truncated, and compressed geometries up to 14.90% exhibited very similar values of the Mach number and potential core length. The 22.35% and 29.80% truncations showed a more substantial reduction in the Mach number of the potential core compared to the MOC. Additionally, the truncated geometries for these two percentages exhibited a slightly larger potential core. A notable point is the compressed geometry of 29.80%, which had a more significant reduction in the Mach number when compared to the truncated geometry of 29.80%.

From another analytical perspective, when the curvilinear geometries are compared to the trapezoidal geometry, the MOC geometry demonstrated a 14.6% increase in the Mach number. The truncated geometries at 7.45%, 14.90%, 22.35%, and 29.80% also showed significant improvements, with gains of 14.3%, 14.2%, 11.5%, and 10.6%, respectively. Moreover, the compressed geometries at 7.45%, 14.9%, 22.35%, and 39.80% also exhibited considerable gains, with increases of 14.7%, 14.2%, 11.7%, and 6.6%, respectively, in comparison to the trapezoidal geometry.

5. CONCLUSION

The variation of the divergent section geometry of the nozzle alters the supersonic jet flow patterns. Truncating the geometry intensifies the oblique shocks incident from the nozzle exit, while compression intensifies the shocks originating from the nozzle throat. Both compressing and truncating the geometry by 7.5% exhibited characteristics similar to the MOC geometry. Truncating the geometry beyond 14.90% led to the occurrence of a normal shock due to the incident shock from the nozzle exit. Compressing the geometry beyond 22.35% resulted in a normal shock from the incident shock at the nozzle throat. Compressing the geometry by 29.80% proved to be more detrimental than truncating it by 29.8%. The curvilinear geometries exhibited higher Mach numbers and potential core lengths compared to the trapezoidal geometry, indicating a greater capacity to generate turbulence in the hot metal at greater distances. In summary, truncated and compressed curvilinear geometries demonstrated advantages over the trapezoidal geometry, offering potential enhancements in nozzle performance.

6. REFERENCES

Allamaprabhu Y, Raghunandan BN, Moríñigo JA. Numerical prediction of nozzle flow separation: Issue of turbulence modeling. Aerospace Science and Technology. 2016;50:31-43.

Anderson JD. Modern compressible flow: with historical perspective. 4th Edition. New York: McGraw-Hill; 2021. Ansys, Inc. 2013. Ansys fluent theory guide. Release 15.0. Canonsburg, PA: ANSYS, Inc.

ANSYS, 2023. Theory Reference. ANSYS, Inc., Pensilvânia, EUA.

Cory Dodson (2023). Minimum Length Nozzle Design Tool (https://www.mathworks.com/matlabcentral/fileexchange/39499-minimum-length-nozzle-design-tool), MATLAB Central File Exchange. Retrieved October 27, 2023.

Cory Dodson (2023). Supersonic Nozzle Design Tool (https://www.mathworks.com/matlabcentral/fileexchange/43212-supersonic-nozzle-design-tool), MATLAB Central File Exchange. Retrieved October 27, 2023.

Fruehan, R. The Making, Shaping, and Treating of Steel: Steelmaking and refining volume. [S.l.] AISE Steel Foundation, 1998. ISBN 9780930767020.

Garajau, Fabrício. Estudo de caso: Desgaste nos bocais supersônicos do bico de lança da aciaria BOF. Orientador: Paulo Roberto Cetlin. 2017. Dissertação de pós-graduação – UFMG, Minas Gerais, 2017.

Hadjadj A, Perrot Y., Verma S. Numerical study of shock/boundary layer interaction in supersonic overexpanded nozzles. Aerospace Science and Technology. 2015;42:158-168.

Li M, Li Q, Kuang SB, Zou Z. Coalescence characteristics of supersonic jets from multi-nozzle oxygen lance in steelmaking BOF. Steel Research International. 2015;86:1517-1529.

Maia, Breno. Efeito da configuração do bico da lança na interação jato-banho metálico em convertedor LD. Orientador: Roberto Tavares. 2007. Dissertação (Mestrado) - UFMG, Minas Gerais, 2007.

Ostlund, J.; MUHAMMAD-KLINGMANN, B. Supersonic Flow Separation with Application to Rocket Engine Nozzles. ASME, [S. l.], p. 143-177, 1 maio 2005. DOI 10.1115/1.1894402. Disponível em: http://asmedigitalcollection.asme.org/appliedmechanicsreviews/article-pdf/58/3/143/5441163/143_1.pdf. Acesso em: 17 set. 2022.

Silveira DCO, Hamadeh H, Pastel K, Huber J-C, Brosse G. Effect of supersonic nozzle design on jet behavior in BOF steelmaking. In: Associação Brasileira de Metalurgia, Materiais e Mineração. Anais do 50º Seminário de Aciaria, Fundição e Metalurgia de Não-Ferrosos; 2019; São Paulo, Brazil. São Paulo: ABM; 2019. p. 302-313.

Storch AP, Furtado HS, Bernabé ACA, Sartim R. Simulação computacional do sopro de oxigênio dos convertedores BOF da ArcelorMittal tubarão. In: Associação Brasileira de Metalurgia, Materiais e Mineração. Anais do 48º Seminário de Aciaria, Fundição e Metalurgia de Não-Ferrosos; 2017; São Paulo, Brazil. São Paulo: ABM; 2017. p. 662-673.

Zapryagaev, Valeriy et al. An experimental and numerical study of a supersonic jet shock-wave structure. NASA STI/Recon Technical Report N, [S.l.], p. 197-191,10 jul. 2002. Disponível em: https://www.researchgate.net/publication/253685784_An_Experimental_and_Numerical_Study_of_A_Supersonic - Jet_Shock-Wave_Structure. Acesso em: 15 jun. 2023.

7. RESPONSIBILITY NOTICE

The authors are the only responsible for the printed material included in this paper.